

1 **Title: Boundary trees offer large carbon sequestration opportunities in Indian croplands**

2 Authors: Siddharth Sachdeva<sup>1,2</sup>, Richard Lee<sup>2</sup>, Sherrie Wang<sup>3,4</sup>, Chandrashekhara Biradar<sup>5</sup>,  
3 David B. Lobell<sup>2,6</sup>

4

5 <sup>1</sup>Emmett Interdisciplinary Program in Environment and Resources, Stanford University,  
6 Stanford, CA 94305, USA

7 <sup>2</sup>Center on Food Security and the Environment, Stanford University, Stanford, CA 94305, USA

8 <sup>3</sup>Institute for Data, Systems, and Society, Massachusetts Institute of Technology, Cambridge,  
9 MA, USA

10 <sup>4</sup>Department of Mechanical Engineering, Massachusetts Institute of Technology, Cambridge,  
11 MA, USA

12 <sup>5</sup>Global Green Growth Company, Bengaluru, Karnataka, India

13 <sup>6</sup>Department of Earth System Science, Stanford University, Stanford, CA 94305, USA

14

15 **Abstract**

16 Agroforestry offers the promise of enhanced CO<sub>2</sub> sequestration, farmer income, climate  
17 resilience, and biodiversity, yet little is known about the current extent or future potential of  
18 specific agroforestry practices. We combine new datasets on 600 million trees and 146 million  
19 farm field boundaries across India to map the extent and potential of boundary plantations, a  
20 specific practice where farmers grow trees on field boundaries. To account for errors in machine  
21 learning predictions of both tree cover and field boundaries, we annotate >4000 high-resolution  
22 images and use prediction-powered inference to construct statistically valid confidence intervals.  
23 We find a national sequestration potential of 3.9 +/- 0.21 Gt of CO<sub>2</sub> for additional boundary trees  
24 in India cropland, with current adoption representing <15% of total potential. Many of the most  
25 promising states for future adoption are also among the poorest in India, suggesting synergies  
26 between climate and poverty goals.

27

28

29

30

31

32

33

34

35

36

37

38

39 Adding trees to agricultural land is often considered one of the most scalable and cost-effective  
40 opportunities for CO<sub>2</sub> removal<sup>1</sup>. Farmland trees also provide many other potential co-benefits,  
41 including food and fodder production, habitat for biodiversity, regulation of microclimate, and  
42 reductions in soil erosion<sup>2</sup>. These co-benefits have driven significant interest among farmers,  
43 scientists, policymakers, and businesses to increase adoption of agroforestry practices.

44  
45 Recent studies have built on global remote sensing tree cover datasets to estimate the current  
46 adoption and future potential of agroforestry broadly<sup>3-5</sup>. For example, Chapman et al.<sup>1</sup> use a  
47 30-meter woody tree cover product to estimate the potential additional CO<sub>2</sub> sequestration in  
48 each country by assuming the current median level of tree cover in each biome represents a  
49 realistic counterfactual level of CO<sub>2</sub> stocks in trees on farmland. Zomer et al.<sup>6</sup> use a global  
50 medium-resolution tree cover product and IPCC tier 1 estimates of CO<sub>2</sub> density to estimate  
51 current CO<sub>2</sub> stocks from agroforestry, with subsequent work<sup>7</sup> using these data to estimate  
52 potential CO<sub>2</sub> sequestration in various adoption scenarios. These studies generally point to a  
53 larger sequestration potential for agroforestry than almost all other natural climate solutions<sup>4</sup>,  
54 though estimates vary widely. For example, Roe<sup>4</sup> estimates technical potential of 5-6 GT CO<sub>2</sub>  
55 year<sup>-1</sup> globally, Griscom estimates maximum potential of 1 GTCO<sub>2</sub> year<sup>-1</sup> globally, and Zomer  
56 estimate from 1.83 to 19 GT CO<sub>2</sub> total potential depending on the adoption scenario.

57  
58 Several limitations of prior studies make it difficult to know with high confidence how much CO<sub>2</sub>  
59 agroforestry can sequester. First, estimates of potential largely depend on low-resolution (>30-  
60 meter) tree cover maps that miss many scattered trees in complex smallholder agricultural  
61 landscapes in the tropics<sup>8</sup>, leading to underestimates of current tree cover and therefore  
62 overestimates of potential additional tree cover. Significant advances in methods and data for  
63 mapping trees at high resolution in agricultural land have been made using remote sensing  
64 satellite imagery, leading to the publication of national<sup>9</sup> and even continental-scale high-  
65 resolution maps<sup>8</sup> of trees in agricultural land, and these can be used to make more accurate  
66 estimates of current and potential tree cover. Second, estimates from previous work use  
67 machine learning generated predictions for remote sensing tree cover, but do not correct for  
68 machine learning prediction errors, which can lead to bias in the estimated potential. Recent  
69 approaches such as prediction-powered inference (PPI) enable the estimation of statistically  
70 valid confidence intervals from machine learning predictions<sup>10,11</sup>, and these approaches should  
71 be used to calibrate estimates of potential tree cover based on machine learning predictions.

72  
73 Third, whereas most studies consider the broad question of adding trees to agricultural land,  
74 often assuming all fields transition to median level of tree cover<sup>7</sup>, understanding is needed at the  
75 level of specific agroforestry practices such as windbreaks, silvopasture, and riparian buffers<sup>12</sup>.  
76 Each practice is appropriate for different types of agricultural systems, crop species, and soil  
77 and climate conditions. For example, silvopasture is feasible in pasture lands and some crop  
78 lands where livestock are the primary source of income, while windbreaks are more common in  
79 croplands where crops are the primary income stream. Existing work estimating potential  
80 sequestration assumes that median levels of tree cover in each landscape represent the  
81 potential adoption scenario for agroforestry, ignoring the role of specific agroforestry practices.  
82 Each agroforestry practice is context-specific, so trying to estimate the adoption or potential of

83 farmland trees without understanding the specific practices in play can lead to misestimation of  
84 both current adoption and future potential of agroforestry.

85  
86 According to prior estimates of CO<sub>2</sub> sequestration potential from agroforestry, India is among the  
87 countries with the largest total CO<sub>2</sub> sequestration potential<sup>4</sup>. Agroforestry has a history as a  
88 traditional agricultural practice in India spanning thousands of years, with a wide diversity of  
89 agroforestry practices in different regions of the country<sup>13</sup>. India was also the first country to  
90 implement a National Agroforestry Policy<sup>14</sup>, so there is clear interest from policy makers on  
91 scaling the adoption of agroforestry. One policy called “Har Medh Par Ped,” translated as “trees  
92 on every field boundary,”<sup>15</sup> incentivized farmers across 20 states to add trees to crop-field  
93 boundaries. <sup>916</sup>This practice of adding trees to crop field boundaries is often referred to as  
94 windbreaks<sup>12</sup>. Importantly, windbreaks do not require taking land away from other crops while  
95 providing significant co-benefits to annual cropping systems including reduce wind damage,  
96 reduced soil erosion, microclimate moderation, providing fodder for livestock, additional income  
97 streams, and habitat for pollinators and other biodiversity. It therefore represents, in our view,  
98 one of the most scalable options among the agroforestry options.

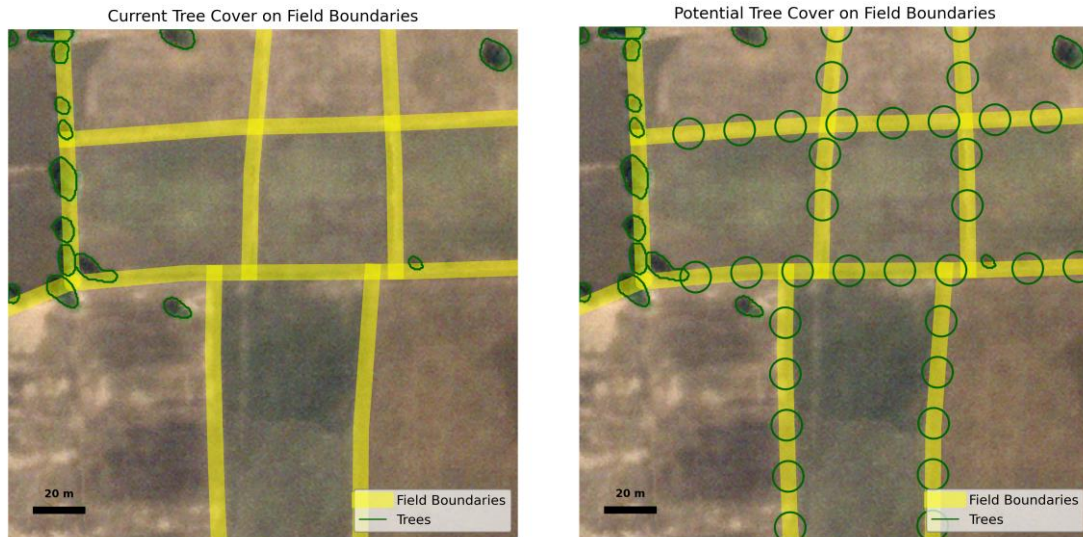
99  
100 Here we aim to estimate how much CO<sub>2</sub> could be sequestered if farmers across India added  
101 trees to field boundaries. Leveraging high resolution datasets on tree cover<sup>9</sup> and field  
102 boundaries<sup>16</sup> that have recently been developed using satellite data and machine learning  
103 approaches, we estimate the current stock and potential additional CO<sub>2</sub> sequestration from  
104 increasing adoption of windbreaks in India.

105  
106  
107

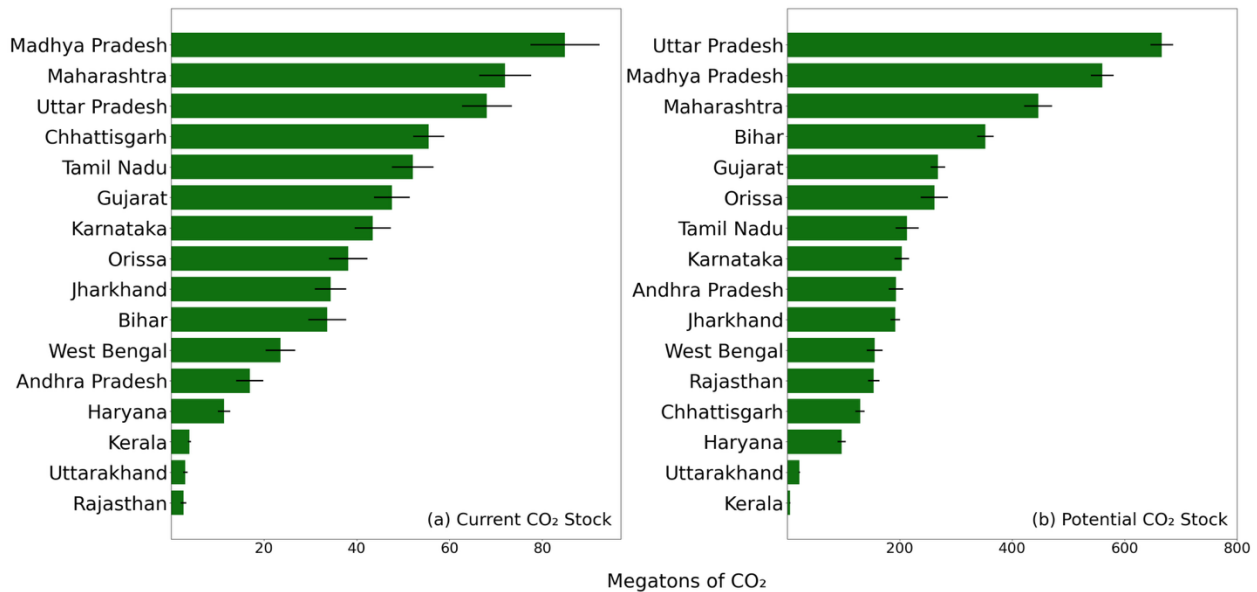
## 108 **Results**

109 For both current and potential tree cover, we consider only areas within 3m of current field  
110 boundaries (see Figure 1). We estimate that existing Indian boundary trees have a total stock of  
111 0.59 +/- 0.05 Gt CO<sub>2</sub> (Figure 2a), with additional potential from trees added to field boundaries of  
112 3.92 +/- 0.21 Gt CO<sub>2</sub> (Figure 2b), using 95% confidence intervals in both cases. Large states  
113 like Maharashtra, Uttar Pradesh, Madhya Pradesh unsurprisingly contain both the largest  
114 current and potential CO<sub>2</sub> stocks.

115

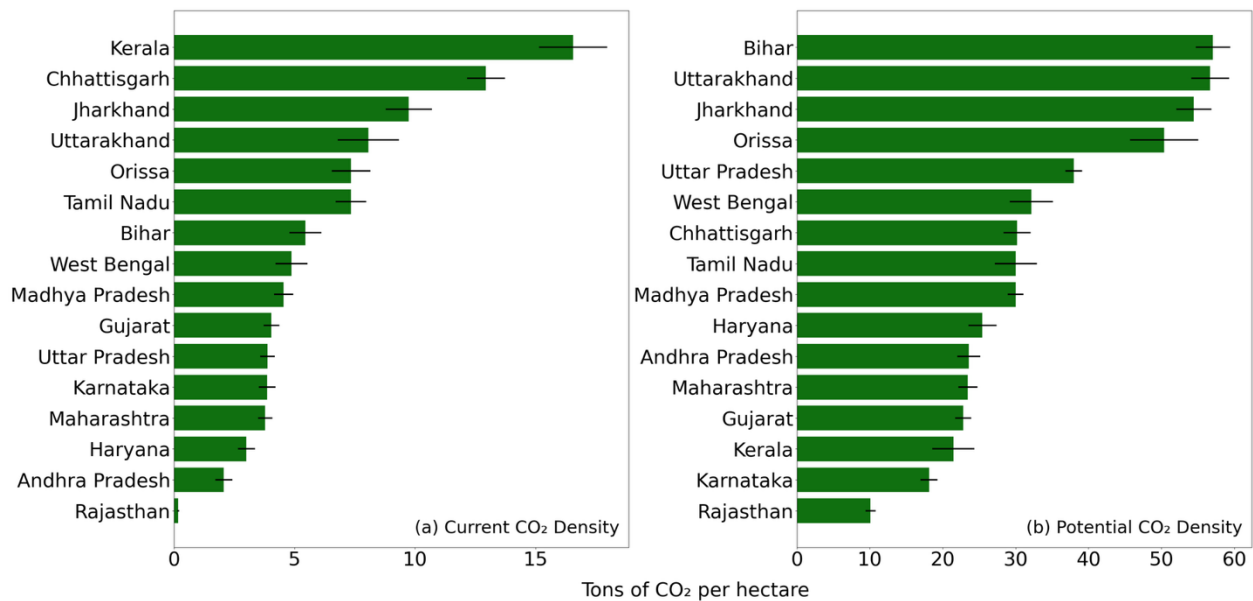


116  
 117 **Figure 1: An Illustration of Border Tree Estimates.** Example 200 x 200 meter satellite image  
 118 with annotated field boundaries (yellow) and tree cover (green) for the current extent of adoption  
 119 (left) and the potential from adding trees to boundaries without trees (right).  
 120



121  
 122 **Figure 2: Current and Potential Total CO<sub>2</sub> Sequestration** a) PPI-adjusted Current CO<sub>2</sub> Stock  
 123 on Field Boundaries by state, with 95% confidence intervals. b) PPI-adjusted CO<sub>2</sub> Sequestration  
 124 Potential by state, with 95% confidence intervals.  
 125

126 We also report estimates for the density of current (Figure 3a) and potential (Figure 3b)  
 127 boundary tree CO<sub>2</sub> stocks to control for the size of different states. Kerala, Tamil Nadu, and  
 128 Jharkhand contain the largest current density of CO<sub>2</sub> stocks, suggesting that both poor and rich  
 129 states can have high boundary tree cover. However, the largest potential density is in poor  
 130 states like Bihar, Jharkhand, and Uttarakhand, indicating significant potential for synergies  
 131 between CO<sub>2</sub> sequestration and poverty alleviation (Table S1).



133

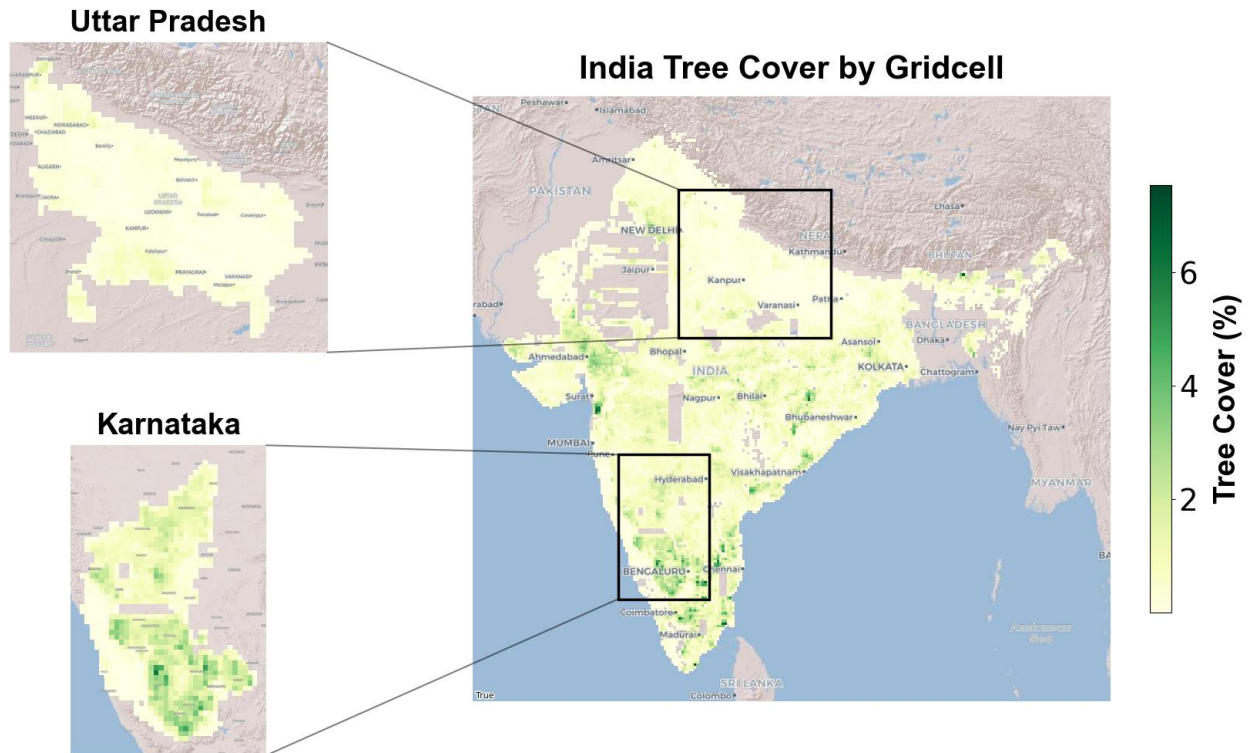
134

135 **Figure 3a: Current and Potential CO<sub>2</sub> Densities** a) PPI-adjusted Current CO<sub>2</sub> Stock Density  
 136 on Field Boundaries by state, with 95% confidence intervals. b) PPI-adjusted CO<sub>2</sub> Sequestration  
 137 Potential Density by state, with 95% confidence intervals.

138

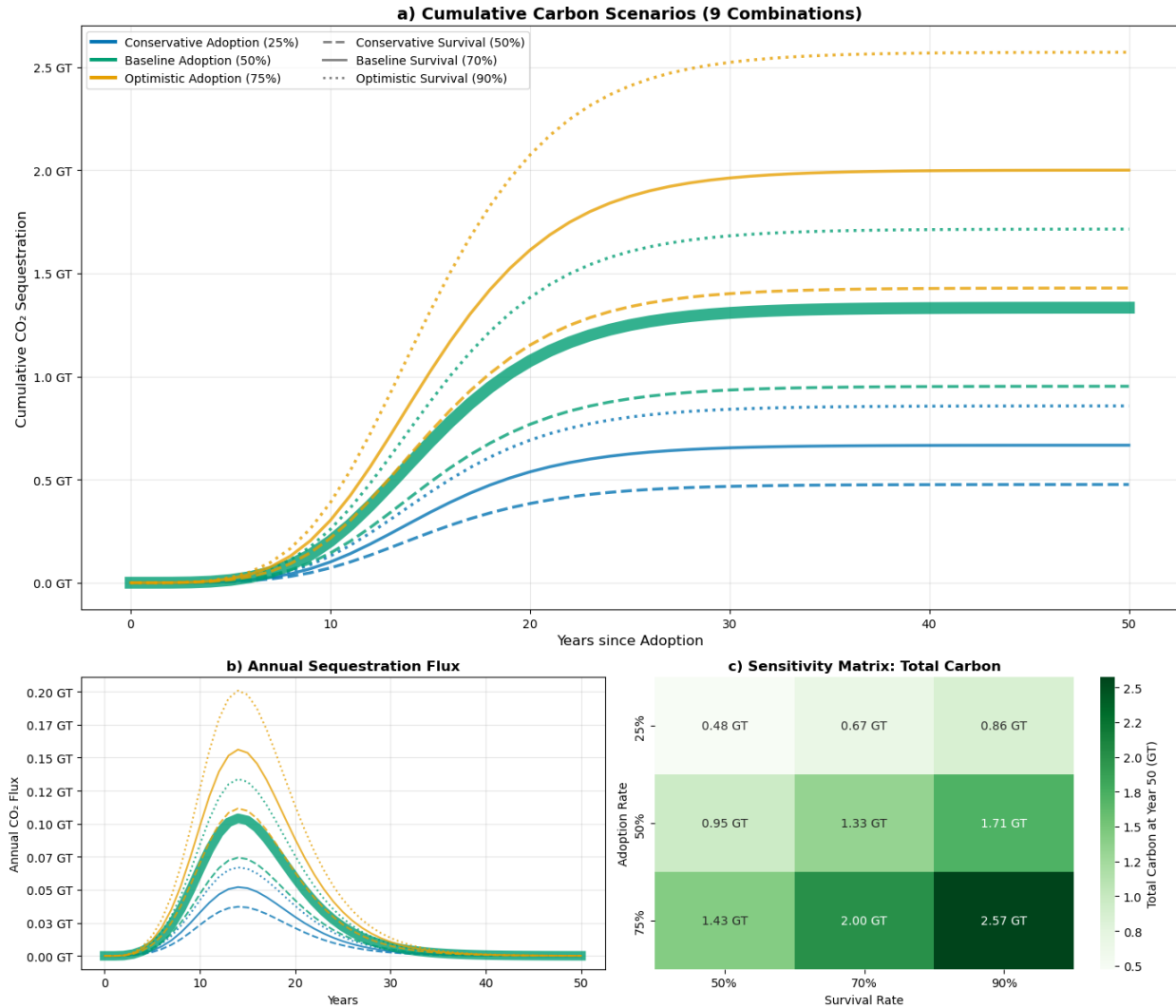
139 A map of our estimates highlights that South India has a significantly higher current adoption  
 140 rate of boundary tree practices than North India (Figure 4). In addition, adoption seems to be  
 141 clustered in specific areas throughout the country, indicating that a farmer is more likely to have  
 142 boundary trees if nearby to other farmers with this practice, perhaps because farmers learn from  
 143 neighbors<sup>17</sup>. This clustering pattern appears at multiple scales and invites future qualitative work  
 144 to understand why these areas have higher adoption rates of boundary trees.

## Current Boundary Tree Cover Percentage in India



145  
146 **Figure 4: Map of Current Boundary Tree Cover in India.** High adoption of this practice is  
147 clustered in specific areas, such as southern Karnataka.  
148

149  
150 We use our estimates of total potential CO<sub>2</sub> sequestration to construct scenarios of varying  
151 levels of adoption of boundary tree practices (25%,50%,75%) and varying levels of tree  
152 mortality (50%,70%,90%), following existing data on tree mortality in India (Figure 5). The level  
153 of adoption is the primary factor driving total potential CO<sub>2</sub> sequestration, even when tree  
154 mortality is 50%. We also observe that annual CO<sub>2</sub> sequestration only increases beyond 100 Mt  
155 after ~10 years in all scenarios, as trees take time to grow, and the majority of CO<sub>2</sub>  
156 sequestration will happen between 10 and 20 years after adoption. However, even in the most  
157 conservative scenarios of mortality and adoption, promoting boundary tree practices still leads  
158 to more than one Gt of CO<sub>2</sub> sequestration for the country of India.



159  
160  
161  
162  
163  
164  
165  
166

**Figure 5: Cumulative and annual carbon sequestration in various adoption scenarios.** Under varying adoption scenarios (25%, 50%, 75%) and varying tree mortality scenarios (50%, 70%, 90%) we report a) Cumulative CO<sub>2</sub> Sequestration Scenarios over over Time, b) Annual sequestration flux, and c) Total CO<sub>2</sub> sequestration Sensitivity Matrix to these varying scenarios

## Discussion

167 Our analysis reveals that boundary plantations in India represent a substantial natural climate  
168 solution that is currently largely untapped. By integrating high-resolution remote sensing with  
169 rigorous statistical correction, we estimate a technical potential for additional carbon  
170 sequestration of 3.9 +/- 0.21 Gt CO<sub>2</sub>. This value is roughly equivalent to 1.4 years of India's total  
171 greenhouse gas emissions, or nearly 11 years of the country's transportation sector  
172 emissions<sup>18</sup>. These findings align with the upper range of estimates for agroforestry potential in  
173 India from previous global studies but offer a crucial refinement: by focusing specifically on field  
174 boundaries, we demonstrate that gigaton-scale removal is possible without competing with food  
175 crops for land. This distinguishes boundary trees from other land-intensive mitigation strategies,

176 such as afforestation or block plantations, making them uniquely viable for India's land-  
177 constrained, smallholder-dominated agricultural system.

178 Methodologically, we present a scalable framework for converting "imperfect" big data into  
179 "policy-grade" evidence. As satellite imagery and machine learning models become ubiquitous,  
180 the risk of propagating prediction errors into policy decisions grows. Our application of PPI<sup>11</sup>  
181 highlights the danger of relying on raw machine learning outputs alone. Without the PPI rectifier,  
182 standard approaches would have underestimated the current CO<sub>2</sub> stock on field boundaries (by  
183 65%) and overestimated the potential CO<sub>2</sub> sequestration on field boundaries (by 59%), leading  
184 to biased overestimates of future potential. By pairing massive but noisy satellite datasets with  
185 small, high-quality "gold standard" samples, we show that it is possible to produce statistically  
186 valid confidence intervals at national scales. This approach can be readily applied to map other  
187 climate-smart practices, such as cover cropping, tillage reduction, or water conservation  
188 structures anywhere in the world where high-resolution training data is scarce but determining  
189 accurate adoption rates is critical.

190 Geographically, our results point to a geographic roadmap for intervention. While states in  
191 South India currently exhibit higher adoption rates, the greatest *potential* for additional  
192 sequestration lies in the northern and eastern plains, particularly in states like Chhattisgarh,  
193 Bihar, and Jharkhand. These regions are characterized by lower current tree densities but high  
194 biophysical suitability for agroforestry. Crucially, these are also some of India's most  
195 economically vulnerable states. Prioritizing these areas for schemes like "Har Medh Par Ped"  
196 could deliver a "triple win": sequestering carbon, enhancing climate resilience against  
197 heatwaves and erosion, and providing new income streams from timber and fodder for low-  
198 income farmers.

199 Finally, while this study establishes the biophysical potential of boundary trees, realizing this  
200 potential requires addressing the socio-economic dimensions of adoption. Our biophysical maps  
201 show where trees can grow, but they do not explain why they are absent. Future research  
202 should prioritize understanding the barriers preventing farmers in high-potential regions from  
203 planting trees—whether it be insecure land tenure, lack of access to quality saplings, or  
204 concerns over competition with crops. Furthermore, our carbon estimates assume survival rates  
205 based on typical growth curves, yet actual sequestration will depend heavily on species  
206 selection and long-term tree management. Integrating these high-resolution spatial estimates  
207 with on-the-ground socio-economic surveys will be essential for designing incentives that  
208 ensure planted trees survive to maturity, transforming this massive theoretical potential into a  
209 permanent climate reality.

## 210 **Methods**

211  
212 To estimate the current extent and additional potential of adding trees to field boundaries for  
213 India, we combine two recently released national-scale high-resolution data products for India: a  
214 dataset on field boundaries released by Wang et al.<sup>19</sup>, and a dataset on tree cover released by  
215 Brandt et al.<sup>9</sup>. Both datasets were derived from applying machine learning models to very high-  
216 resolution satellite data to generate smallholder field-scale geospatial data products. Although  
217 they represent the best available data, they contain sufficient errors to necessitate explicit  
218 adjustment in our analysis, which we achieve using prediction-powered inference (described  
219 below).  
220

221 Data

222 *Smallholder Field Boundaries*

223 Wang et al.<sup>19</sup> train a machine learning model to predict field boundaries from both Airbus 1.5-  
224 meter imagery and PlanetScope 4.8-meter imagery. They performed manual annotation on high-  
225 resolution satellite imagery of >10,000 fields sampled from France and India to train and  
226 evaluate their model, achieving IoU of 0.86 in India. Here we developed an India wide dataset of  
227 field boundaries by applying this model to 1.5 meter imagery from airbus across India,  
228 generating 146 million field boundaries. There were issues with airbus imagery in some regions,  
229 so some regions have been ignored, largely concentrated in Northwest India, and these gaps  
230 are visible in Figure 4.

231

232 *Farmland Tree Cover*

233 Brandt et al.<sup>9</sup> train a machine learning model to predict pixel-level tree cover from PlanetScope  
234 3-meter imagery, enabling them to achieve near individual tree-level spatial resolution for tree  
235 cover. Again, they use manual annotations of high-resolution satellite imagery to train and  
236 evaluate their model achieving an F1-score of 0.65.

237

238 *Other data sources*

239 To focus only on fields that represent cropland, we use the ESRI LULC 10-meter land cover  
240 map to filter out non-cropland pixels, which has 90.2% precision in detecting cropland on a  
241 biome-stratified dataset for the world. We also leave out states with an area smaller than 30,000  
242 square km. as their contribution to the national CO<sub>2</sub> sequestration potential is negligible to the  
243 total potential.

244

245 Estimating Current and Potential Boundary Tree CO<sub>2</sub> Sequestration

246 To estimate the current extent and future potential CO<sub>2</sub> sequestration from adding trees to field  
247 boundaries, we estimate both the current area of field boundaries and the area of boundary  
248 trees at the state-level for 17 states of India, leaving out small states.

249

250 *Computing current extent of field boundaries*

251 We convert the predicted field boundary polylines to polygons by adding a 3-meter buffer. For  
252 each state, we compute the sum of the areas of these buffered polygons to estimate the total  
253 area of field boundaries, representing the total potential area for adding trees to field  
254 boundaries.

255

256 *Computing current extent of boundary tree cover*

257 We take the 3-meter tree cover raster from Brandt et al.<sup>9</sup> and identify all pixels with both 1) tree  
258 cover confidence greater than a threshold of 0.5 and 2) a 3-meter radius field boundary  
259 overlapping with the pixel. We then sum all such pixels to compute the total area of boundary  
260 tree cover.

261

262 *Correcting for Errors in ML-derived products for field boundaries and tree cover*

263 Because ML-derived predictions are always imperfect, both the field boundaries and tree cover  
264 products contain errors which can bias estimates of the current extent of boundary tree cover.

265 To account for these errors, we leveraged the prediction-powered inference ++ framework<sup>10</sup>, an  
 266 approach for generating statistically valid confidence intervals for a parameter of interest using  
 267 ML-derived predictions. This process requires having a gold-standard dataset in which the  
 268 ground truth values of the quantity of interest are present alongside the ML-derived predictions.  
 269 This paired dataset of ground truth values the ML predictions enables one to compute a rectifier  
 270 and a standard deviation, following the algorithm from PPI, shown below.

- 271
- 272 **Input:** labeled data  $(X, Y)$ , unlabeled features  $\tilde{X}$ , predictor  $f$ , error level  $\alpha \in (0, 1)$
- 273 1:  $\hat{\theta}^{\text{PP}} \leftarrow \tilde{\theta}^f - \hat{\Delta} := \frac{1}{N} \sum_{i=1}^N f(\tilde{X}_i) - \frac{1}{n} \sum_{i=1}^n (f(X_i) - Y_i)$   $\triangleright$  prediction-powered estimator
- 274 2:  $\hat{\sigma}_f^2 \leftarrow \frac{1}{N} \sum_{i=1}^N (f(\tilde{X}_i) - \tilde{\theta}^f)^2$   $\triangleright$  empirical variance of imputed estimate
- 275 3:  $\hat{\sigma}_{f-Y}^2 \leftarrow \frac{1}{n} \sum_{i=1}^n (f(X_i) - Y_i - \hat{\Delta})^2$   $\triangleright$  empirical variance of empirical rectifier
- 276 4:  $w_\alpha \leftarrow z_{1-\frac{\alpha}{2}} \sqrt{\frac{\hat{\sigma}_{f-Y}^2}{n} + \frac{\hat{\sigma}_f^2}{N}}$   $\triangleright$  normal approximation

---

277 **Output:** prediction-powered confidence set  $C_\alpha^{\text{PP}} = (\hat{\theta}^{\text{PP}} \pm w_\alpha)$

278

279 *Constructing groundtruth annotations for tree cover and field boundaries.*

280 To construct our gold-standard set, we leverage high-resolution 50-cm Planet Skysat images to  
 281 annotate both individual tree crowns and field boundaries (Figure 1). This resolution is more  
 282 than sufficient to accurately resolve field boundaries and individual tree crowns. Specifically, we  
 283 trained an annotator to label all tree crowns and boundary polylines for 200 200 m x 200 m  
 284 images for every state in India, totaling more than 4000 annotated images. To ensure high-  
 285 quality, we perform double annotation for 200 images from across India and measure inter-  
 286 annotator agreement, achieving IOU of 89%.

287

288 *Using groundtruth images and state-level estimates to construct PPI intervals for each state*

289 Given our annotated set of skysat images, we compute the predicted tree cover and boundary  
 290 areas for these images using the same data products described above, which yields paired  
 291 groundtruth and predicted values for boundary tree cover and boundary area in each satellite  
 292 image. If we treat boundary area, boundary tree cover, and potential additional boundary tree  
 293 cover within a 200 m x 200 m square as our parameters of interest within the PPI framework,  
 294 we can use our 200 paired values of  $Y$  ("ground truth) and  $Y_{\text{hat}}$  (predicted values) for each  
 295 parameter to construct a statistically valid confidence interval . We then multiply the point  
 296 estimates and upper and lower bounds for the densities by the number of 200 m x 200 m  
 297 squares in the whole state to convert our estimates to total values for the whole state.

298

299 *Computing Potential CO<sub>2</sub> Sequestration from Boundary Trees*

300 To convert our tree cover area estimates to CO<sub>2</sub> stocks requires estimates of CO<sub>2</sub> density.  
 301 Panwar et al.<sup>20</sup> conducted a comprehensive review of CO<sub>2</sub> densities in agroforestry systems in  
 302 different regions and practices of India. As expected, the CO<sub>2</sub> densities are higher in wetter  
 303 biomes than in dryer biomes. Because we do not have CO<sub>2</sub> densities for every region in India,

304 we make the simplifying assumption that CO<sub>2</sub> density linearly increases with the amount of  
305 rainfall within an observed range, and we use the minimum and maximum CO<sub>2</sub> densities found  
306 in this study to define this range in both CO<sub>2</sub> density and rainfall. We use block plantation CO<sub>2</sub>  
307 densities because we are only considering the area on which there are trees rather than the  
308 whole farm. We compute average CO<sub>2</sub> densities for each state using average annual rainfall.  
309 Specifically, we set the range of CO<sub>2</sub> density to be between 52 tons ha<sup>-1</sup> and 139 tons ha<sup>-1</sup> which  
310 are the lowest and highest CO<sub>2</sub> densities in block plantations that occur in the driest and wettest  
311 parts of India respectively<sup>20</sup>. The CO<sub>2</sub> densities are shown in Supplementary Figure 1,  
312 averaging close to 100 tons ha<sup>-1</sup>, which is similar to the CO<sub>2</sub> densities used in Roe et al.<sup>4</sup> and  
313 Griscom et al. for similar regions. To construct confidence intervals of current and potential CO<sub>2</sub>  
314 sequestration from boundary trees, we simply multiply the point estimate and standard  
315 deviations by the CO<sub>2</sub> densities for that state.

316

### 317 *Forecasting CO<sub>2</sub> Sequestration Under Various Adoption and Mortality Scenarios*

318 Given our estimate of total potential CO<sub>2</sub> sequestration, we constructed different scenarios to  
319 forecast realistic CO<sub>2</sub> sequestration over time while varying levels of adoption and levels of tree  
320 mortality. We assume that tree growth follows the Chapman-Richard growth function<sup>20</sup> below,  
321 where B<sub>max</sub> is the maximum CO<sub>2</sub> a tree can hold which we derive from our total potential  
322 calculation, k is the growth rate which we set at 0.25, and m is the lag phase during which tree  
323 growth is fairly slow .

324

$$B_t = B_{max} \cdot (1 - e^{-k \cdot t})^m$$

325

326 We use a value of m = 3 , which is a common value for fast growing agroforestry tree species  
327 and assume adoption follows the Bass Diffusion model with a logistic S curve below. A<sub>max</sub> is  
328 the maximum potential adoption rate, which we vary over a conservative, baseline, and  
329 optimistic scenario of 25%, 50%, and 75%, and we assume the adoption period is 15 years,  
330 after which the farmers who would adopt border trees have already done so. We also account  
331 for tree mortality with conservative, baseline, and optimistic scenarios of 50%, 70%, and 90%.<sup>21</sup>

332

333

$$A(t) = \frac{A_{max}}{1 + e^{-c(t-t_{mid})}}$$

334

## 335 Bibliography

336

337

338

1. Chapman M, Walker WS, Cook-Patton SC, et al. Large climate mitigation potential from adding trees to agricultural lands. *Glob Change Biol.* 2020;26(8):4357-4365. doi:10.1111/gcb.15121

- 339 2. Verchot LV, Van Noordwijk M, Kandji S, et al. Climate change: linking adaptation and  
340 mitigation through agroforestry. *Mitig Adapt Strateg Glob Change*. 2007;12(5):901-918.  
341 doi:10.1007/s11027-007-9105-6
- 342 3. Dhyani SK, Ram A, Dev I. Potential of Agroforestry Systems in Carbon Sequestration in  
343 India. *Social Science Research Network*. Preprint posted online July 1, 2015:3755763.  
344 Accessed December 8, 2025. <https://papers.ssrn.com/abstract=3755763>
- 345 4. Roe S, Streck C, Beach R, et al. Land-based measures to mitigate climate change:  
346 Potential and feasibility by country. *Glob Change Biol*. 2021;27(23):6025-6058.  
347 doi:10.1111/gcb.15873
- 348 5. Griscom BW, Adams J, Ellis PW, et al. Natural climate solutions. *Proc Natl Acad Sci*.  
349 2017;114(44):11645-11650. doi:10.1073/pnas.1710465114
- 350 6. Zomer RJ, Neufeldt H, Xu J, et al. Global Tree Cover and Biomass Carbon on Agricultural  
351 Land: The contribution of agroforestry to global and national carbon budgets. *Sci Rep*.  
352 2016;6(1):29987. doi:10.1038/srep29987
- 353 7. Zomer RJ, Bossio DA, Trabucco A, et al. Global carbon sequestration potential of  
354 agroforestry and increased tree cover on agricultural land. *Circ Agric Syst*. 2022;2(1):1-10.  
355 doi:10.48130/CAS-2022-0003
- 356 8. Brandt M, Tucker CJ, Kariryaa A, et al. An unexpectedly large count of trees in the West  
357 African Sahara and Sahel. *Nature*. 2020;587(7832):78-82. doi:10.1038/s41586-020-2824-5
- 358 9. Brandt M, Gominski D, Reiner F, et al. Severe decline in large farmland trees in India over  
359 the past decade. *Nat Sustain*. 2024;7(7):860-868. doi:10.1038/s41893-024-01356-0
- 360 10. Angelopoulos AN, Duchi JC, Zrnic T. PPI++: Efficient Prediction-Powered Inference.  
361 Prediction-powered inference | Science. Accessed December 8, 2025.  
362 <https://www.science.org/doi/10.1126/science.adi6000>
- 363 12. Gene Garrett HE, Buck L. Agroforestry practice and policy in the United States of America.  
364 *For Ecol Manag*. 1997;91(1):5-15. doi:10.1016/S0378-1127(96)03884-4
- 365 13. Pandey DN. Multifunctional agroforestry systems in India. *Curr Sci*. 2007;92(4):455-463.
- 366 14. Chavan SB, Keerthika A, Dhyani SK, Handa AK, Newaj R, Rajarajan K. National  
367 Agroforestry Policy in India: a low hanging fruit. *Curr Sci*. 2015;108(10):1826-1834.
- 368 15. Schemes for Agro-Forestry. Accessed February 11, 2026.  
369 <https://www.pib.gov.in/Pressreleaseshare.aspx?PRID=1705520&reg=3&lang=2>
- 370 16. Unlocking Large-Scale Crop Field Delineation in Smallholder Farming Systems with  
371 Transfer Learning and Weak Supervision | MDPI. Accessed February 11, 2026.  
372 <https://www.mdpi.com/2072-4292/14/22/5738>

373 17. Maertens A. Who Cares What Others Think (or Do)? Social Learning and Social Pressures  
374 in Cotton Farming in India. *Am J Agric Econ.* 2017;99(4):988-1007.  
375 doi:10.1093/ajae/aaw098

376 18. India - Countries & Regions - IEA. Accessed February 11, 2026.  
377 <https://www.iea.org/countries/india/emissions>

378 19. Wang S, Waldner F, Lobell DB. Unlocking Large-Scale Crop Field Delineation in  
379 Smallholder Farming Systems with Transfer Learning and Weak Supervision. *Remote Sens.*  
380 2022;14(22). doi:10.3390/rs14225738

381 20. Panwar P, Mahalingappa DG, Kaushal R, et al. Biomass Production and Carbon  
382 Sequestration Potential of Different Agroforestry Systems in India: A Critical Review.  
383 *Forests.* 2022;13(8):1274. doi:10.3390/f13081274

384 21. Zhao-gang L, Feng-ri L. The generalized Chapman-Richards function and applications to  
385 tree and stand growth. *J For Res.* 2003;14(1):19-26. doi:10.1007/BF02856757

386 22. Dhyani SK, Tripathi RS. Tree growth and crop yield under agrisilvicultural practices in north-  
387 east India. *Agrofor Syst.* 1998;44(1):1-12. doi:10.1023/A:1006176303162

388 23. Handbook of Statistics on Indian States - Reserve Bank of India. Accessed April 10, 2026.  
389 [https://rbi.org.in/Scripts/AnnualPublications.aspx?head=Handbook%20of%20Statistics%20o](https://rbi.org.in/Scripts/AnnualPublications.aspx?head=Handbook%20of%20Statistics%20on%20Indian%20States)  
390 [n%20Indian%20States](https://rbi.org.in/Scripts/AnnualPublications.aspx?head=Handbook%20of%20Statistics%20on%20Indian%20States)

391

392

393

394

395

396

397

398

399

400

401

402

403

404

405

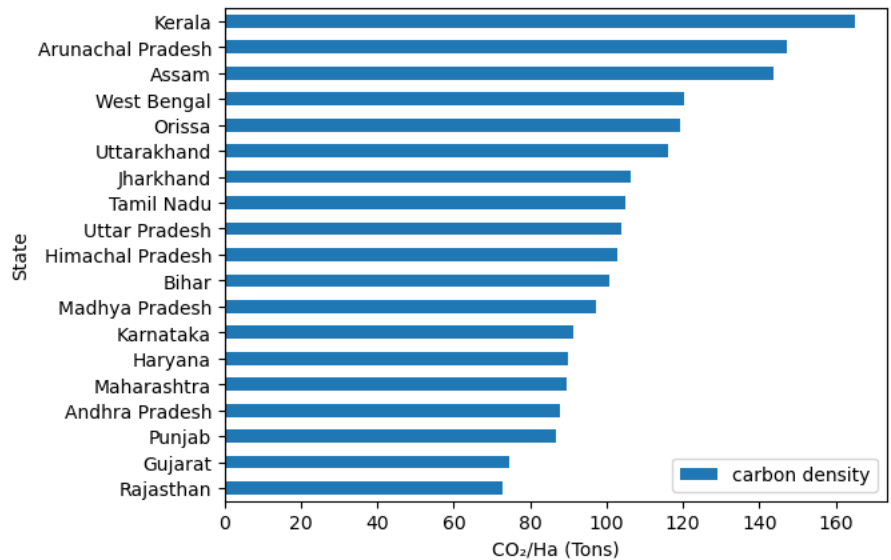
406 **Supplements**

407

State	Per Capita Income (Nominal USD)	Current Boundary Tree Carbon	Potential Boundary Tree Carbon
Karnataka	\$4,445	15.46	72.45
Haryana	\$4,372	12.03	101.81
Tamil Nadu	\$4,269	29.37	120.06
Gujarat	\$4,069	16.19	91.22
Maharashtra	\$3,858	15.13	93.8
Kerala	\$3,837	66.23	85.8
Uttarakhand	\$3,572	32.27	226.74
Andhra Pradesh	\$3,264	8.27	94.3
Rajasthan	\$2,264	0.7	40.36
West Bengal	\$2,188	19.48	128.62
Odisha	\$2,166	29.39	201.5
Madhya Pradesh	\$1,889	18.19	120
Chhattisgarh	\$1,799	51.77	120.79
Jharkhand	\$1,400	38.95	217.79
Uttar Pradesh	\$1,298	15.53	151.97
Bihar	\$807	21.82	228.27

408 **Supplementary Table 1:** Per-capita GDP by state (from Reserve Bank of India Handbook of  
 409 Statistics on Indian States) along with boundary tree cover density estimates from this study. <sup>22</sup>

410



411 **Supplementary Figure 1:** Carbon densities assigned for each state which we estimate using  
 412 existing evidence on carbon sequestration of agroforestry of various biomes in India along with  
 413 the rainfall level for each state.  
 414  
 415

416  
 417  
 418  
 419  
 420  
 421  
 422  
 423  
 424  
 425  
 426  
 427  
 428  
 429  
 430  
 431  
 432  
 433  
 434  
 435  
 436

437

438

439

440

441

442

443